AIMS Materials Science, 5(1): 145–155.
DOI: 10.3934/matersci.2018.1.145
Received: 29 December 2017
Accepted: 26 February 2017
Published: 05 March 2018

http://www.aimspress.com/journal/Materials

Research article

Synthesis, structural characterization and thermal stability of a 2D layered Cd(II) coordination polymer constructed from squarate ($C_4O_4^{2-}$) and 2,2'-*bis*(2-pyridyl)ethylene (2,2'-bpe) ligands

Chih-Chieh Wang[1,*], Yu-Fan Wang[1], Szu-Yu Ke[1], Yanbin Xiu[1], Gene-Hsiang Lee[2], Bo-Hao Chen[3] and Yu-Chun Chuang[3,*]

[1] Department of Chemistry, Soochow University, Taipei 11102, Taiwan
[2] Instrumentation Center, National Taiwan University, Taipei 10617, Taiwan
[3] National Synchrotron Radiation Research Center, Hsinchu 30076, Taiwan

* **Correspondence:** Email: ccwang@scu.edu.tw; chuang.yc@nsrrc.org.tw; Tel: +886-2-28819471 ext 6828; Fax: +886-2-28811053.

Abstract: A mixed-ligands Cd(II) coordination polymer, [Cd(2,2'-bpe)(C_4O_4)(H_2O)$_2$] (**1**) (2,2'-bpe = 1,2-*bis*(2-pyridyl)ethylene; $C_4O_4^{2-}$ = dianion of squaric acid), has been synthesized and structurally characterized by single-crystal X-ray diffraction method. The coordination environment of Cd(II) ions in compound **1** is six-coordinate bonded to four oxygen atoms from two $\mu_{1,3}$-squarate ($C_4O_4^{2-}$) and two water molecules, and two nitrogen atoms from two 2,2'-bpe ligands. The squarate and 2,2'-bpe both act as bridging ligands with *bis*-monodentate coordination modes, connecting the Cd(II) ions to form a two-dimensional (2D) layered metal-organic framework (MOF). Adjacent 2D layers are then arranged in an ABAB parallel non-interpenetrating manner to construct its three dimensional (3D) supramolecular network. Intra- and inter-layers hydrogen bonding interactions between the $C_4O_4^{2-}$ and water molecules in **1** provide an extra-stabilization energy on the construction of its 3D supramolecular network. The thermal stability of **1** is studied and discussed in details by TG analysis and *in-situ* PXRD measurement.

Keywords: coordination polymer; metal-organic framework; hydrogen bond; squarate; Cd(II)

1. Introduction

The design and synthesis of new open-framework mixed-ligands coordination polymers have been the focus of current chemical and new material research. Of particular importance is the ability of the organic linkers to influence profoundly the structures of synthesized products, and to direct their formation with specific structures and potential applications [1–5], such as magnetism, host–guest chemistry, shape specificity and catalysis. Squarate dianions ($C_4O_4^{2-}$), the de-protonated form of squaric acid (3,4-dihydroxycyclobut-3-ene-1,2-dione, $H_2C_4O_4$) has been paid much attention to, from the crystal engineering point of view, as the building units with template capacity to set up the assembly procedure of stable one-, two-, and three-dimensional (1D, 2D and 3D) crystalline materials. In the relevant approach, the squarate serves as a unique ligand, which possesses a four-membered cyclic aromatic structure characterized by extensive π electron delocalization all over carbon and oxygen atoms which has been widely used as a polyfunctional ligand, such as hydrogen bonding or π–π interactions, for the construction of extended supramolecular architecture and also used as a bridging ligand with various coordination modes (μ_2 to μ_8 bridges) to build up many coordination polymers with novel extended networks, including 1D chain, 2D layer, 3D cube- and cage-like frameworks [6–47]. The planar D_{4h} structures of squarate have been well established on their metal salts or complexes. In our previous study, we have reported several metal-squarate MOFs associated with N,N-donor bridging/chelating type co-ligands, like 4,4'-bipyridine (4,4'-bipy), and 1,2-*bis*(4-pyridyl)ethane (dpe) [43–47]. With our continuous effort on the study of metal-squarate coordination polymers, the structural topology of metal ions with the used co-ligands, 1,2-*bis*(2-pyridyl)ethylene (2,2'-bpe), seems to be interesting and worth to be further investigated. Focusing on this approach, we report here the synthesis, structural characteristics and thermal stability of a coordination polymer, $[Cd(2,2'\text{-bpe})(C_4O_4)(H_2O)_2]_n$ (**1**), in which the squarate and 2,2'-bpe both act as the bridging ligands with $\mu_{1,3}$-coordination and *bis*-monodentate mode, respectively, to build up its 2D extended layered MOF. The intra- and inter-layer hydrogen boning interaction plays an important role on the construction of its 3D supramolecular architecture.

2. Materials and method

2.1. Materials and physical techniques

All chemicals were of reagent grade and were used as commercially obtained without further purification. Elementary analyses (carbon, hydrogen and nitrogen) were performed using a Perkin-Elmer 2400 elemental analyzer. The infrared spectra was recorded on a Nicolet Fourier Transform IR, MAGNA-IR 500 spectrometer in the range of 500–4000 cm^{-1} using the KBr disc technique. Thermogravimetric analysis (TGA) was performed on a computer-controlled *Perkin-Elmer* 7 Series/UNIX TGA7 analyzer. Single-phased powder samples were loaded into alumina pans and heated with a ramp rate of 5 °C/min from room temperature to 800 °C under nitrogen flux.

*2.2. Synthesis of $[Cd(C_4O_4)(2,2\text{-bpe})(H_2O)_2]_\infty$ (**1**)*

An ethanol/H_2O solution (1:1, 3 mL) of $H_2C_4O_4$ (5.8 mg, 0.05 mmol) was added to an

ethanol/water (1:1, 6 mL) solution of $Cd(NO_3)_2 \cdot 4H_2O$ (15.5 mg, 0.05 mmol) and 1,2-*bis*(2-pyridyl)ethylene (18.2 mg, 0.05 mmol) at room temperature. After standing for one week, light-brown block crystals of **1** (yield, 12.1 mg; 54.6%) were obtained which are suitable for X-ray diffraction analysis. Anal. Calc. for $C_{14}H_{12}N_2O_6Cd_1$ (**1**): C 43.41, N 6.33, H 3.19; Found: C 43.69, N 5.95, H 2.91. IR (KBr pellet): ν = 3278 (s), 3083 (m), 1711 (w), 1601 (s), 1520 (vs), 1438 (m), 1341 (m), 1222 (m), 1159(m), 1096 (m), 1008 (m), 966 (m), 780 (m), 694 (m), 637 (m) cm^{-1}.

2.3. Crystallographic data collection and refinements

Single-crystal structural analysis was performed on a Siemens SMART diffractomer with a CCD detector with Mo Kα radiation (λ = 0.71073 Å) at room temperature. A preliminary orientation matrix and unit cell parameters were determined from 3 runs of 15 frames each, each frame corresponds to a 0.3° scan in 10 s, following by spot integration and least-squares refinement. For each structure, data were measured using ω scans of 0.3° per frame for 20 s until a complete hemisphere had been collected. Cell parameters were retrived using SMART [48] software and refined with SAINT [49] on all observed reflections. Data reduction was performed with the SAINT [49] software and corrected for Lorentz and polarization effects. Absorption corrections were applied with the program SADABS [50]. Direct phase determination and subsequent difference Fourier map synthesis yielded the positions of all non-hydrogen atoms, which were subjected to anisotropic refinements. For compound **1**, all hydrogen atoms were generated geometrically ($C–H_{sp^2}$ = 0.93 Å) with the exception of the hydrogen atoms of the coordinated water molecules, which were located in the difference Fourier map with the corresponding positions and isotropic displacement parameters being refined. The final full-matrix, least-squares refinement on F^2 was applied for all observed reflections [I > 2σ(I)]. All calculations were performed using the SHELXTL-PC V 5.03 software package [51]. Crystallographic data and details of data collections and structure refinements of compound **1** are listed in Table 1.

Table 1. Crystal data and refinement details of **1**.

compound **1**			
Chemical formula	$C_{16}H_{14}N_2O_8Cd$	Molecular formula	442.71
Crystal system	Monoclinic	Space group	$P\ 2_1/c$
a/Å	8.3983(6)	α(°)	90.0
b/Å	12.3407(9)	β(°)	103.827(1)
c/Å	8.3960(6)	γ(°)	90.0
V/Å^3	844.95(11)	Z	2
T (K)	295(2)	D_{calcd} (g cm^{-3})	1.740
μ (mm^{-1})	1.327	θ range (deg)	2.50–27.48
total no. of data collected	6342	no. of unique data	1931
no. of obsd data ($I > 2\sigma(I)$)	1792	R_{int}	0.0163
R_1, wR_2 ($I > 2\sigma(I)$)[1]	0.0180, 0.0437	R_1, wR_2 (all data)[1]	0.0200, 0.0452
refine params	116	GOF[2]	0.898

[1] $R_1 = \Sigma||F_o - F_c||/\Sigma|F_o|$; $wR_2(F^2) = [\Sigma w|F_o^2 - F_c^2|^2/\Sigma w(F_o^4)]^{1/2}$;

[2] $GOF = [\Sigma[w(F_o^2 - F_c^2)]^2/(N_{obs} - N_{para})]^{1/2}$

CCDC1819496 for **1** contains the supplementary crystallographic data for this paper. These data can be obtained free of charge at www.ccdc.cam.ac.uk/conts/retrieving.html [or from the Cambridge Crystallographic Data Centre, 12, Union Road, Cambridge CB2 1EZ, UK; Fax: (internet.) +44-1223/336-033; E-mail: deposit@ccdc.cam.ac.uk].

2.4. In situ X-ray powder diffraction

Variable temperature synchrotron powder X-ray diffraction data were collected at BL01C2 powder diffraction beamline in National Synchrotron Radiation Research Center. The powder sample was packed into a glass capillary and heated by a heating gun with ramp rate in 10 degree/minute. The X-ray energy was used at 12 keV (wavelength = 1.03321 Å). The *in-situ* powder diffraction data were recorded on a Mar3450 image plate with 72 seconds exposure time. The data calibration and integration were performed by GSAS-II program [52], where diffraction angle is calibrated based on the standard powder sample of LaB_6.

3. Results and discussion

3.1. Synthesis and IR spectroscopy

Compound **1** was synthesized by direct mixing of Cd(II) salts, 2,2'-bpe ligands and squaric acid ($H_2C_4O_4$) with stoichiometric molar ratio of 1:1:1. The infrared spectrum shows a broad band in the region 3000–3400 cm^{-1}, which can be assigned to the stretching vibration, ν(O–H) of the water molecules. The most relevant IR features are those associated with the chelating squarate ligands. The peak at 1711 cm^{-1} is assigned to the uncoordinated carbonyl groups, which exhibits a double bond character. The coordinated C–O groups of squarate are characterized by medium absorptions at 1601 cm^{-1}. A very strong and broad band centered at around 1520 cm^{-1}, which is attributed to vibrational modes representing mixtures of C–O and C–C stretching motions and is in agreement with the characteristic of the $(CO)_n^{2-}$ salts [53].

*3.2. Structural description of $[Cd(C_4O_4)(2,2'\text{-bpe})(H_2O)_2]_n$ (**1**)*

The crystal structure of **1** is determined with a 3D supramolecular network being constructed from 2D-layered MOFs. The Cd(1) lies in a distorted octahedral environment and locates at the inversion center, consisting of two nitrogen atoms from 2,2'-bpe ligand, with the bond distance of Cd(1)–N(1) = 2.400(1) Å and four oxygen atoms from two bridging squarate ligands and two water molecules with the bond distances of Cd(1)–O(1) = 2.265(1), Cd(1)–O(3) = 2.324(1) Å as shown in Figure 1a. The related bond lengths and angles around the Cd(II) ion are listed in Table 2. The squarate and 2,2'-bpe both act as a bridging ligand with $\mu_{1,3}$-*bis*-monodentate and *bis*-monodentate coordination modes, respectively, leading the formation of a 2D layered MOF (Figure 1b) with the quadrilateral grid as the basic fundamental building unit. The pore size of the quadrilateral grids based on the Cd···Cd separations are approximately 8.396(1) × 8.398(1) Å *via* the bridges of squarate and 2,2'-bpe, respectively. The 2D MOF of **1** can be viewed in a simplified way using TOPOS [54,55] as a four-connected uninodal net with the point symmetry (Schläfli symbol) $\{4^4.6^2\}$. Adjacent 2D layers are arranged in a parallel ABAB manners to complete its 3D supramolecular

network (Figure 1c). Hydrogen bonding interaction plays an important role on the stabilization of the 3D supramolecular network (yellow dashed lines shown in Figure 2c). In the crystal packing, the coordinated water molecules (O(3)) are held together with the uncoordinated oxygen atoms (O(2)) of squarate ($C_4O_4^{2-}$) by means of one intra-layer O–H···O hydrogen bond with O···O distances of 2.708(5) Å and the other inter-layer O–H···O hydrogen bond with O···O distances of 2.803(5) Å, respectively, on the further stabilization of its 3D supramolecular architecture. Related bond distances and angles of O–H···O hydrogen bonds are listed in Table 3.

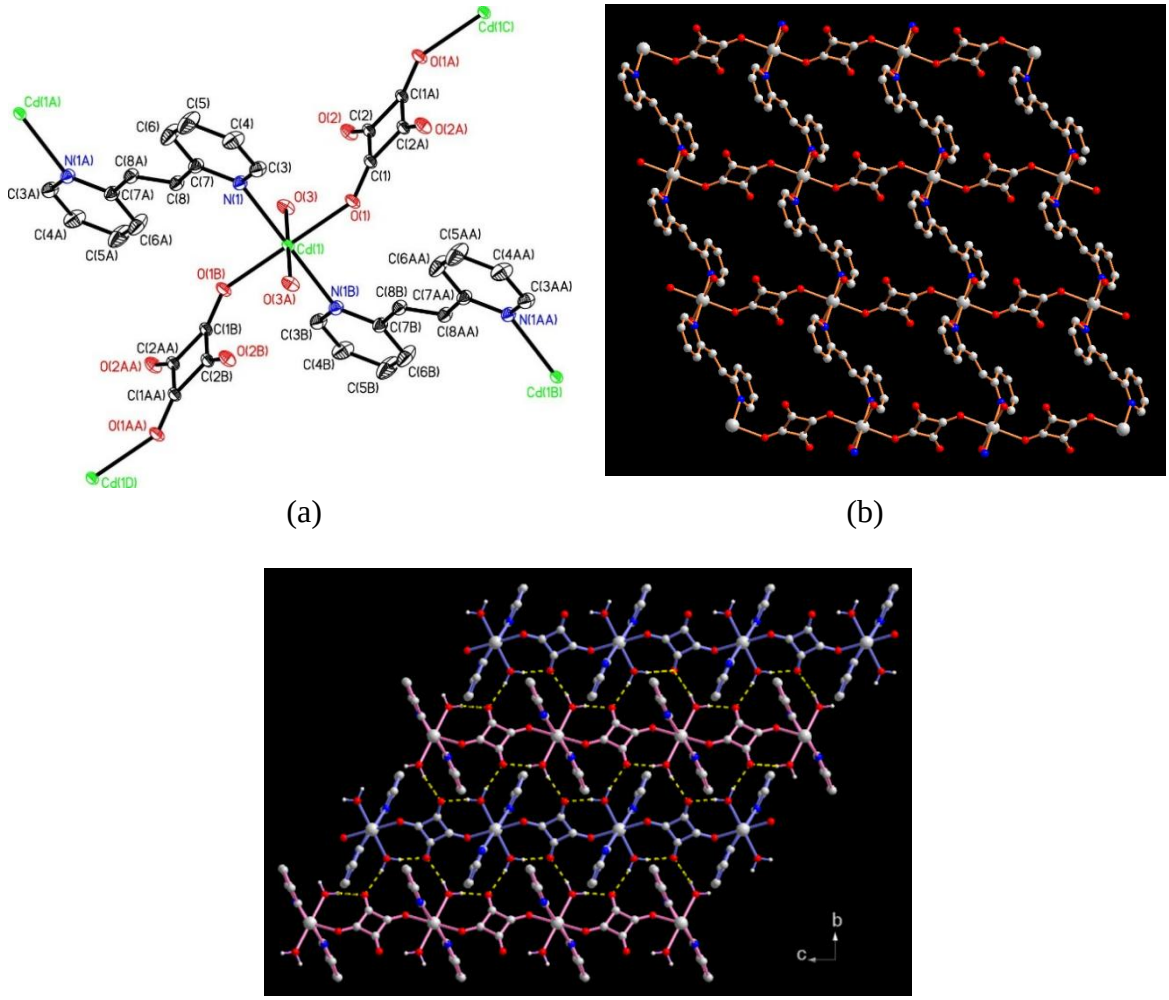

(a) (b)

(c)

Figure 1. (a) Coordination environment of the Cd(II) ion in **1** with atom labelling scheme (ORTEP drawing, 30% thermal ellipsoids). Symmetry codes used to generate equivalent atoms A: −x + 1, y + 3/2, −z + 1/2; B: −x + 1, y + 3/2, −z + 3/2; AA: x, y, z + 1 for squarate ligand and A: −x, y + 3/2, −z + 3/2; B: −x + 1, y + 3/2, −z + 3/2; AA: x + 1, y, z for 2,2'-bpe ligand. (b) The 2D layered MOF of **1** *via* the bridges of squarate and 2,2'-bpe (Larger gray ball for Cd atom; red ball for oxygen atom; blue ball for nitrogen atom and smaller gray ball for carbon atom). (c) The 3D supramolecular network viewing along the *c* axis with the yellow lashed lines for intra- and inter-layer hydrogen bonds between the uncoordinated oxygen atoms (O(2)) of squarate and hydrogen atoms of water molecules (O(3)).

Table 2. Bond lengths (Å) and angles (°) around Cd(II) ion in **1**.[1]

compound **1**			
Cd(1)–O(1)	2.265(1)	Cd(1)–O(1)^{i}	2.265(1)
Cd(1)–O(3)	2.324(1)	Cd(1)–O(3)^{i}	2.324(1)
Cd(1)–N(1)	2.4000(1)	Cd(1)–N(1)^{i}	2.400(1)
O(1)^{i}–Cd(1)–O(1)	180.0	O(1)^{i}–Cd(1)–O(3)^{i}	93.04(4)
O(1)–Cd(1)–O(3)^{i}	86.96(4)	O(1)^{i}–Cd(1)–O(3)	86.96(4)
O(1)–Cd(1)–O(3)	93.04(4)	O(3)^{i}–Cd(1)–O(3)	180.0
O(1)^{i}–Cd(1)–N(1)^{i}	85.26(5)	O(1)–Cd(1)–N(1)^{i}	94.74(5)
O(3)^{i}–Cd(1)–N(1)^{i}	92.00(4)	O(3)–Cd(1)–N(1)^{i}	88.00(4)
O(1)^{i}–Cd(1)–N(1)	94.74(5)	O(1)–Cd(1)–N(1)	85.26(5)
O(3)^{i}–Cd(1)–N(1)	88.00(4)	O(3)–Cd(1)–N(1)	92.00(4)
N(1)^{i}–Cd(1)–N(1)	180.0		

[1] Symmetry transformations used to generate equivalent atoms: i = −x, −y, −z.

Table 3. The O–H···O hydrogen bonds for **1**.[1]

D–H···A	D–H (Å)	H···A (Å)	D···A (Å)	∠ D–H···A (°)
O(3)–H(3A)···O(2)^{i}	0.88(7)	1.99(7)	2.803(2)	168(6)
O(3)–H(3B)···O(2)	0.86(7)	1.84(7)	2.708(2)	171(6)

[1] Symmetry transformations used to generate equivalent atoms: i = x, −y + 1/2, −z + 1/2.

*3.3. Thermal-stability of **1** by thermogravimetric analysis (TGA) and in-situ powder X-ray diffraction measurement (PXRD)*

To assess the thermal stability and structural variation as a function of the temperature, thermogravimetric analysis (TGA) and *in-situ* temperature dependent XRD measurements of **1** were performed on single-phase polycrystalline samples. TGA associated with *in-situ* temperature dependent XRD measurements agree well with the crystallographic observation. During the heating process, the TG analysis (Figure 2a) revealed that compound **1** underwent a two-step weight loss and thermally stable up to 83.5 °C. The first weight loss of 8.8% (calc 8.2%) corresponded to the loss of coordinated water molecules was occurred in the range of approximate 83.5–119.1 °C. In the temperature range of approximate 119.1–228.2 ℃, **1** was stable without any weight lost. On further heating, these samples slowly decrease from 228 ℃ to 360 ℃, but decrease rapidly from 360 ℃ to 450 ℃. The first mass drop may be attributed to the structure transformation after removing the coordination water molecules from Cd(II) center. We expect the un-coordinated oxygen atom of squarate ligand in **1** will coordinate to the Cd(II) and create a rigid 3D structure after the removal of coordinated water molecules in the de-hydrated form. The slow mass drop between 228 to 360 ℃ might come from a small part of sample decomposition in the 3D structure. Above 360 ℃, the structure cannot sustain anymore and a rapid mass-loss is attributed to the sample decomposition process. The thermal stability of the materials was further investigated by *in-situ* powder X-ray diffractometry (see Figure 2b). The powder crystalline structure at room temperature is matching well to its single crystal structure. From room temperature to 140 °C, the crystal structure maintained well and no phase transition occurred. Above 170 °C, a phase transition was observed and the

structure is stable even at 380 °C. The cell parameters from the temperature-variable PXRD patterns were obtained by using indexing program, Dicvol, and listed in the Table 4. During the heating process from room temperature to 170 ℃, the cell volume increases step by step. The *a*, *c* axis lengths and beta angles are changed slightly. However, the *b* axis is stretched obviously. The *b* axis is correlated the 2D layer distance. We strongly suspected the extremely stable structure is still a framework system. Based on the TGA result, the two coordinated water molecules were removed. We propose a preliminary model that the non-coordinated oxygen atoms of squarate ligands were chelated on the open active site of Cd(II) ions after the removal of coordinated water molecules. The O(2) of **1** replace the O(3) position and form a five-member ring to stabilize the 3D de-hydrated framework. We try to index the cell and solve the structure through simulation annealing method. Unfortunately, the diffraction data sets above 170 ℃ cannot be indexed due to the broad diffraction peaks and cannot afford enough information to obtain accurate structure.

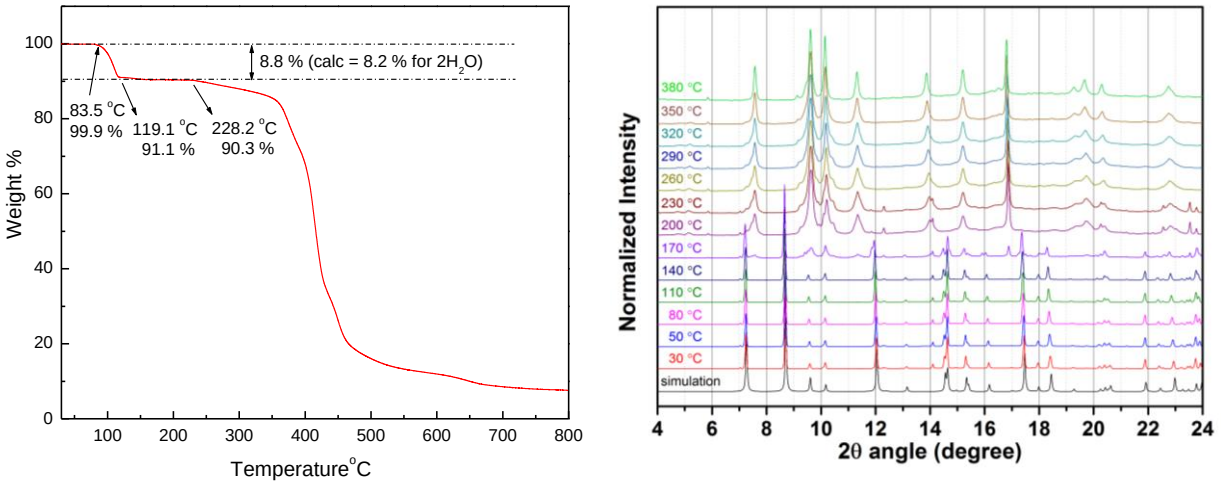

(a) (b)

Figure 2. (a) Thermogravimetric analysis (TGA) of **1**. (b) *In-situ* PXRD patterns of **1** at different temperatures (30–380 ℃) and simulated PXRD pattern of **1** from single-crystal X-ray diffraction data.

Table 4. Cell parameters from *in-situ* synchrotron powder XRD.

Temperature (℃)	*a* (Å)	*b* (Å)	*c* (Å)	β (°)	Volume (Å^3)
30	8.411(3)	12.3475(3)	8.4190(1)	103.701(1)	849.474(3)
50	8.419(7)	12.3779(5)	8.4133(1)	103.721(1)	851.726(7)
80	8.411(2)	12.3858(3)	8.4173(1)	103.622(1)	852.222(2)
110	8.421(5)	12.4041(8)	8.4120(1)	103.617(1)	853.976(5)
140	8.421(2)	12.4363(4)	8.4230(1)	103.498(1)	857.742(2)
170	8.443(11)	12.4646(12)	8.4178(1)	103.208(1)	862.443(11)

4. Conclusions

A mixed-ligands 3D supramolecular network, [Cd(C_4O_4)(2,2'-bpe)(H_2O)$_2$] (**1**), built up by 2D-layered MOFs *via* the bridges of squarate and 2,2-bpe ligands with *bis*-monodentate coordination

modes has been successfully synthesized and structurally characterized. Adjacent 2D layers were then self-assembled *via* the parallel arrangement to form a 3D supramolecular network. Intra- and inter-layer hydrogen bonding interactions between the uncoordinated oxygen atoms of squarate and coordinated water molecules in the framework provide extra-energy on the stabilization of the 3D supramolecular architecture. TGA and *in-situ* powder X-ray diffraction (PXRD) measurements are in accordance with the crystallographic observations, and the result provide evidence that **1** has quite high thermo-stability that keep their crystalline forms up to 228 ℃.

Acknowledgments

The authors wish to thank the Ministry of Science and Technology and Soochow University, Taiwan for financial support.

Conflict of interest

The authors declare that there is no conflict of interest regarding the publication of this manuscript.

References

1. Chen B, Xiang S, Qian G (2010) Metal–Organic Frameworks with Functional Pores for Recognition of Small Molecules. *Accounts Chem Res* 43: 1115–1124.
2. Liu FL, Kozlevčar B, Strauch P, et al. (2015) Robust Cluster Building Unit: Icosanuclear Heteropolyoxocopperate Templated by Carbonate. *Chem Eur J* 21: 18847–18854.
3. Wang XP, Chen WM, Qi H, et al. (2017) Solvent-Controlled Phase Transition of a Co^{II}-Organic Framework: From Achiral to Chiral and Two to Three Dimensions. *Chem Eur J* 23: 7990–7996.
4. Wang Z, Li XY, Liu LW, et al. (2016) Beyond Clusters: Supramolecular Networks Self-Assembled from Nanosized Silver Clusters and Inorganic Anions. *Chem Eur J* 22: 6830–6836.
5. Yuan S, Deng YK, Sun D (2014) Unprecedented Second-Timescale Blue/Green Emissions and Iodine-Uptake-Induced Single-Crystal-to-Single-Crystal Transformation in Zn^{II}/Cd^{II} Metal–Organic Frameworks. *Chem Eur J* 20: 10093–10098.
6. Khan MI, Chang YD, Chen Q, et al. (1994) Synthesis and Characterization of Binuclear Oxo–Vanadium Complexes of Carbon Oxoanion Ligands. Crystal Structures of the Binuclear Vanadium(IV) Complex $(NH_4)[V_2O_2(OH)(C_4O_4)_2(H_2O)_3]\cdot H_2O$, of the Mixed-Valence Vanadium(V)/Vanadium(IV)–Squarate Species $[(n\text{-}C_4H_9)_4N][V_2O_3(C_4O_4)_2(H_2O)_3]\cdot 3H_2O$ and $[(C_4H_9)_4N]_4[V_4O_6(C_4O_4)_5(H_2O)_4]\cdot 6H_2O$, and of the Binuclear Vanadium(IV)–Oxalate Species $[V_2O_2Cl_2(C_2O_4)(CH_3OH)_4]\cdot 2Ph_4PCl$. *Inorg Chem* 33: 6340–6350.
7. Chen Q, Liu S, Zubieta J (1990) Coordination Chemistry of Polyoxomolybdates: The Structure of a Dodecanuclear Molybdate Cage Incorporating Hydrogen Squarate Ligands, $[(C_4H_9)_4N]_4[Mo_{12}O_{36}(C_4O_4H)_4]\cdot 10Et_2O$. *Angew Chem Int Edit* 29: 70–72.
8. Lee CR, Wang CC, Wang Y (1996) Structural relationship of various squarates. *Acta Crystallogr B* 52: 966–975.

9. Bouayad A, Brouca-Cabarrecq C, Trombe JC, et al. (1992) Lanthanide(III)-copper(II) squarates: synthesis, crystal structure, magnetism and thermal behaviour of $[La_2Cu(C_4O_4)_4(H_2O)_{16}]\ 2H_2O$ and $[Gd_2Cu(C_4O_4)4(H_2O)_{12}]2H_2O$. *Inorg Chim Acta* 195: 193–201.
10. Petit JF, Gleizes A, Trombe JC (1990) Lanthanide(III) squarates 1. Five families of compounds obtained from aqueous solutions in an open system. Crystal structure and thermal behaviour. *Inorg Chim Acta* 167: 51–68.
11. Trombe JC, Petit JF, Gleizes A (1990) Lanthanide(III) squarates 2. High diversity of rare coordination modes of the squarate anion in a series of weakly hydrated cerium(III) squarates prepared by pseudo-hydrothermal methods. *Inorg Chim Acta* 167: 69–81.
12. Bouayad A, Trombe JC, Gleizes A (1995) Barium-copper(II) oxocarbon compounds: synthesis, crystal structures and thermal behaviours of $[Ba(H_2O)_5][Cu(C_2O_4)_2(H_2O)]$ and $[Ba(C_4O_4)_{0.5}(H_2O)_2]_2[Cu(C_4O_4)_2(H_2O)_2]$. *Inorg Chim Acta* 230: 1–7.
13. Trombe JC, Sabadie L, Millet P (2002) Synthesis and crystal structure of $La(H_2O)(C_2O_4)_2\ (CN_3H_6)$ and of $[Nd(H_2O)]_2(C_2O_4)_4\ (NH_4)(CN_3H_6)$. *Solid State Sci* 4: 1199–1028.
14. Trombe JC, Sabadie L, Millet P (2002) Hydrothermal synthesis and structural characterization of Fe(II)-squarate $Fe_2(OH)_2(C_4O_4)$. *Solid State Sci* 4: 1209–1212.
15. Soules R, Dahan F, Laurent JP, et al. (1988) A novel coordination mode for the squarate ligand [dihydroxycyclobutenedionate(2–)]: synthesis, crystal structure, and magnetic properties of catena-diaqua(2,2'-bipyridyl)-μ-(squarato-O^1,O^2)-nickel(II) dehydrate. *J Chem Soc Dalton Trans* 587–590.
16. Beneto M, Soto L, Garcia-Lozano J, et al. (1991) Crystal and molecular structure and properties of the first characterized copper(II) one-dimensional polymer containing mepirizole [4-methoxy-2-(5-methoxy-3-methyl-1H-pyrazol-1-yl)-6-methylpyrimidine]. *J Chem Soc Dalton Trans* 1057–1061.
17. Hall LA, Williams DJ, Menzer S, et al. (1997) The Complexing Properties of 1-Aminosquarate Derivatives with Lead. *Inorg Chem* 36: 3096–3101.
18. Alleyne BD, Hall LA, Hosein HA, et al. (1998) Hydrogen-bonding interactions in the series of complexes $[M(C_4O_4)(OH_2)_2(dmf)_2]$ and $[M(C_4O_4)(OH_2)_4]$ (M = Mn, Co, Ni, Cu, Zn). *J Chem Soc Dalton Trans* 3845–3850.
19. Crispini A, Pucci D, Aiello I, et al. (2000) Synthesis and crystal structure of dinuclear cyclopalladated 1,2- and 1,3-bridged squarato complexes. *Inorg Chim Acta* 304: 219–223.
20. Lin KJ , Lii KH (1997) Halozeotypes: a New Generation of Zeolite-Type Materials. *Angew Chem Int Edit* 36: 2076–2077.
21. Lai SF, Cheng CY, Lin KJ (2001) Hydrothermal synthesis of a thermally stable poroussupramolecular π–π framework: $[\{Co_2(C_{12}H_8N_2)_4(\mu\text{-}C_4O_4)(OH_2)_2\}C_4O_4]\ 8H_2O$. *Chem Commun* 1082–1083.
22. Grove H, Sletten J, Julve M, et al. (2001) Syntheses, crystal structures and magnetic properties of one- and two-dimensional pap-containing copper(II) complexes (pap = pyrazino[2,3- f][4,7]phenanthroline). *J Chem Soc Dalton Trans* 259–265.
23. Nather C, Greve J, Jeβ I (2002) New Coordination Polymer Changing Its Color upon Reversible Deintercalation and Reintercalation of Water: Synthesis, Structure, and Properties of Poly[Diaqua-(μ2-Squarato-O,O')-(μ2-4,4'-Bipyridine-N,N')- Manganese(II)] Trihydrate. *Chem Mater* 14: 4536–4542.

24. Piggott PMT, Hall LA, White AJP, et al. (2003) Attempted Syntheses of Lanthanide(III) Complexes of the Anisole- and Anilinosquarate Ligands. *Inorg Chem* 42: 8344–8352.
25. Yang BP, Mao JG (2005) New Types of Metal Squarato-phosphonates: Condensation of Aminodiphosphonate with Squaric Acid under Hydrothermal Conditions. *Inorg Chem* 44: 566–571.
26. Maji TK, Mostafa G, Sain S, et al. (2001) Construction of a 3D array of cadmium(II) using squarate as a building block. *CrystEngComm* 3: 155–158.
27. Konar S, Corbella M, Zangrando E, et al. (2003) The first unequivocally ferromagnetically coupled squarato complex: origin of the ferromagnetism in an interlocked 3D Fe(II) system. *Chem Commun* 1424–1425.
28. Manna SC, Zangrando E, Ribas J, et al. (2005) Squarato-bridged polymeric networks of iron(II) with N-donor coligands: Syntheses, crystal structures and magnetic properties. *Inorg Chim Acta* 358: 4497–4504.
29. Ghosh AK, Ghoshal D, Zangrando E, et al. (2006) Structural diversity in manganese squarate frameworks using N,N-donor chelating/bridging ligands: syntheses, crystal structures and magnetic properties. *Dalton Trans* 1554–1563.
30. Heinl U, Hinse P, Mattes RZ (2001) Oxalato- und Quadratato-Komplexe hochkoordinierter Metallionen: Die Raumnetzstrukturen von $La_2(C_2O_4)(C_4O_4)_2(H_2O)_8 \cdot 2{,}5H_2O$ und $K[Bi(C_2O_4)_2] \cdot 5H_2O$. *Anorg Allg Chem* 627: 2173–2177.
31. Habenschuss M, Gerstein BC (1974) An x-ray, spectroscopic, and magnetic study of the structure of nickel squarate dihydrate, $NiC_4O_4 \cdot 2H_2O$. *J Chem Phys* 61: 852–860.
32. Hosein HA, Hall LA, Lough AJ, et al. (1998) Attempted Syntheses of Transition Metal and Lanthanide (Dialkylamino)squarates. The Hydrolysis Problem. *Inorg Chem* 37: 4184–4189.
33. Hosein HA, Jaggernauth H, Alleyne BD, et al. (1999) First-Row Transition-Metal Complexes of the 1-Methoxycyclobutenedionate(1−) Ion. *Inorg Chem* 38: 3716–3720.
34. Spandl J, Brüdgam I, Hartl H (2001) Solvothermal Synthesis of a 24-Nuclear, Cube-Shaped Squarato-oxovanadium(IV) Framework: $[N(nBu)_4]_8[V_{24}O_{24}(C_4O_4)_{12}(OCH_3)_{32}]$. *Angew Chem Int Edit* 40: 4018–4020.
35. Mukherjee PS, Konar S, Zangrando E, et al. (2002) Synthesis, crystal structure and magneto-structural correlation of two bi-bridging 1D copper(II) chains. *J Chem Soc Dalton Trans* 3471–3476.
36. Neeraj S, Noy ML, Rao CNR, et al. (2002) Sodalite networks formed by metal squarates. *Solid State Sci* 4: 1231–1236.
37. Dan M, Rao CNR (2003) An open-framework cobalt oxalato-squarate containing a ligated amine. *Solid State Sci* 5: 615–620.
38. Kurmoo M, Kumagai H, Chapman KW, et al. (2005) Reversible ferromagnetic–antiferromagnetic transformation upon dehydration–hydration of the nanoporous coordination framework, $[Co_3(OH)_2(C_4O_4)_2] \cdot 3H_2O$. *Chem Commun* 3012–3014.
39. Gandara F, Gomez-Lor B, Iglesias M, et al. (2009) A new scandium metal organic framework built up from octadecasil zeolitic cages as heterogeneous catalyst. *Chem Commun* 2393–2395.
40. Gutschke SOH, Molinier M, Powell AK, et al. (1997) Hydrothermal Synthesis of Microporous Transition Metal Squarates: Preparation and Structure of $[CO_3(\mu^3\text{-}OH)_2(C_4O_4)_2] \cdot 3H_2O$. *Angew Chem Int Edit* 36: 991–992.

41. Yufit DS, Price DJ, Howard JAK, et al. (1999) New type of metal squarates. Magnetic and multi-temperature X-ray study of di-hydroxy(μ6-squarato)manganese. *Chem Commun* 1561–1562.
42. Robl C, Weiss AZ (1987) Darstellung und Struktur von $Ag_2C_4O_4$. *Anorg Allg Chem* 546: 161–168.
43. Yang CH, Chou CM, Lee GH, et al. (2003) Self-assembly of two mixed-ligands metal-organic coordination polymers, $[M^{II}_2(DPA)_2(C_4O_4)(C_2O_4)]$ (M = Cu, Zn). *Inorg Chem Commun* 6: 135–140.
44. Wang CC, Yang CH, Tseng SM, et al. (2004) A new moisture-sensitive metal-coordination solids $\{[Cd(C_4O_4)(bipy)(H_2O)_2]\ 3H_2O\}_\infty$ (bipy = 4,4'-bipyridine). *Inorg Chim Acta* 357: 3759–3764.
45. Wang CC, Yang CH, Lee GH, et al. (2005) Syntheses, Structures, and Magnetic Properties of Two 1D, Mixed-Ligand, Metal Coordination Polymers, $[M(C_4O_4)(dpa)(OH_2)]$ (M = Co^{II}, Ni^{II}, and Zn^{II}; dpa = 2,2'-dipyridylamine) and $[Cu(C_4O_4)(dpa)(H_2O)]_2$ (H_2O). *Eur J Inorg Chem* 1334–1342.
46. Wang CC, Yang CH, Lee GH (2006) Hydrothermal Synthesis and Structural Characterization of Two pH-Controlled Cd–Squarate Coordination Frameworks, $[Cd_2(C_4O_4)_{2.5}(H_2O)_4]$ (dpaH) $\cdot 1.5(H_2O)$ and $[Cd(C_4O_4)(dpa)(OH_2)]$ (dpa = 2,2'-dipyridylamine). *Eur J Inorg Chem* 820–826.
47. Wang CC, Tseng SM, Lin SY, et al. (2007) Assemblies of Two Mixed-Ligand Coordination Polymers with Two-Dimensional Metal−Organic Frameworks Constructed from M(II) Ions with Croconate and 1,2-Bis-(4-pyridyl)ethylene (M = Cd and Zn). *Cryst Growth Des* 7: 1783–1790.
48. Smart V (1995) 4.043 Software for CCD Detector System, Siemens Analytical Instruments Division, Madison, WI, USA.
49. Saint V (1995) 4.035 Software for CCD Detector System, Siemens Analytical Instruments Division, Madison, WI, USA.
50. Sheldrick GM (1993) Program for the Refinement of Crystal Structures, University of Göttingen, Göttingen, Germany.
51. Sheldrick GM (1995) SHELXTL 5.03 (PC-Version), Program Liberary for Structure Solution and Molecular Graphics, Siemens Analytical Instruments Division, Madison, WI, USA.
52. Toby BH, Von Dreele RB (2013) GSAS-II: the genesis of a modern open-source all purpose crystallography software package. *J Appl Crystallogr* 46: 544–549.
53. Ito M, Weiss RJ (1963) New Aromatic Anions. IV. Vibrational Spectra and Force Constants for $C_4O_4^{-2}$ and $C_5O_5^{-2}$. *J Am Chem Soc* 85: 2580–2584.
54. Blatov VA, Shevchenko AP, Serezhkin VN (2000) TOPOS3.2: A new version of the program package for multipurpose crystal-chemical analysis. *J Appl Crystallogr* 33: 1193–1193.
55. Blatov VA, Carlucci L, Ciani G, et al. (2004) Interpenetrating metal–organic and inorganic 3D networks: A computer-aided systematic investigation. Part I. Analysis of the Cambridge structural database. *CrystEngComm* 6: 377–395.

AIMS Press